

Article

Modeled Forest Conversion Influences Humid Tropical Watershed Hydrology More than Projected Climate Change

Taylor Joyal ^{1,*} , Alexander K. Fremier ²  and Jan Boll ³ ¹ School of Earth and Sustainability, Northern Arizona University, Flagstaff, AZ 86011, USA² School of the Environment, Washington State University, Pullman, WA 99164, USA³ Department of Civil and Environmental Engineering, Washington State University, Pullman, WA 99164, USA

* Correspondence: taylor.joyal@nau.edu; Tel.: +1-928-523-1588

Abstract: In the humid tropics, forest conversion and climate change threaten the hydrological function and stationarity of watersheds, particularly in steep terrain. As climate change intensifies, shifting precipitation patterns and expanding agricultural and pastoral land use may effectively reduce the resilience of headwater catchments. Compounding this problem is the limited long-term monitoring in developing countries for planning in an uncertain future. In this study, we asked which change, climate or land use, more greatly affects stream discharge in humid tropical mountain watersheds? To answer this question, we used the process-based, spatially distributed Soil Moisture Routing model. After first evaluating model performance ($N_s = 0.73$), we conducted a global sensitivity analysis to identify the model parameters that most strongly influence simulated watershed discharge. In particular, peak flows are most influenced by input model parameters that represent shallow subsurface soil pathways and saturation-excess runoff while low flows are most sensitive to macropore hydraulic conductivity, soil depth and porosity parameters. We then simulated a range of land use and climate scenarios in three mountain watersheds of central Costa Rica. Our results show that deforestation influences streamflow more than altered precipitation and temperature patterns through changes in first-order hydrologic hillslope processes. However, forest conversion coupled with intensifying precipitation events amplifies hydrological extremes, reducing the hydrological resilience to predicted climate shifts in mountain watersheds of the humid tropics. This finding suggests that reforestation can help mitigate the effects of climate change on streamflow dynamics in the tropics including impacts to water availability, flood pulses, channel geomorphology and aquatic habitat associated with altered flow regimes.

Keywords: watershed hydrology model; humid tropics; land use; climate change; hydrological resilience

Citation: Joyal, T.; Fremier, A.K.; Boll, J. Modeled Forest Conversion Influences Humid Tropical Watershed Hydrology More than Projected Climate Change. *Hydrology* **2023**, *10*, 160. <https://doi.org/10.3390/hydrology10080160>

Academic Editor: Genxu Wang

Received: 29 April 2023

Revised: 18 July 2023

Accepted: 22 July 2023

Published: 31 July 2023



Copyright: © 2023 by the authors. Licensee MDPI, Basel, Switzerland. This article is an open access article distributed under the terms and conditions of the Creative Commons Attribution (CC BY) license (<https://creativecommons.org/licenses/by/4.0/>).

1. Introduction

Departure from long-term climate averages has occurred more rapidly in the tropics than anywhere on Earth [1]. Contrary to the large seasonal climate swings at high latitudes, tropical latitudes experience a narrow range of annual climatic fluctuation, making these regions especially sensitive to climate change. In particular, the precipitation regime of the humid tropics is characterized by frequent high-magnitude, high-intensity events with less pronounced interannual hydrological variability than higher latitudes [2,3]. Climate predictions for the tropics forecast increased interannual variability [1,4]. This expected departure from historical climate patterns includes even more intense precipitation events interrupted by drought conditions [1,4–8].

Predicted climate swings may amplify existing hydrological impacts linked to land use, especially when coupled with mountain topography more prone to runoff than infiltration. Agricultural, pastoral, and urban land use in mountain watersheds of the humid tropics is expanding faster and with less regulation of human development than mountainous terrain in temperate and semi-arid regions [2,3]. Published research suggests that land

use/land cover change (LUCC) projections used by the IPCC may be low relative to observations, particularly tropical deforestation rates [9,10]. Moreover, tropical regions include most developing nations with limited capital for monitoring water resources and climate change [11], and monitoring efforts in decline [3]. Yet, scientific emphasis on temperate regions has left a gap in knowledge of tropical watershed dynamics, including how these coupled human–natural systems respond to climate change in conjunction with expanding land use [3].

As climate change intensifies, the interaction of increasingly non-stationary climate regimes with modified vegetation and soil conditions associated with expanded agricultural and pastoral land use threatens the intrinsic resilience of watersheds to maintain services to the ecosystems and societies they support [12,13]. Particularly, the resilience of headwater-dependent human communities can be directly impacted by disturbances that affect watershed hydrology. In this way, intact forests in the headwaters represent a mechanism to maintain system resilience by helping to moderate flood flows and maintain low flows [14–17]. Thus, to better inform land use planning, there is value in estimating the relative magnitude of the moderating effects of forest cover under changing ecohydrological conditions in regions experiencing unprecedented climatic trajectories.

Clearing forest cover for agricultural and pastoral land use influences the amount and timing of water moving through a watershed by altering vegetation, organic litter, soil depth and structure, and consequently, the pathways that water travels to reach stream channels (Figure 1; see [14]). In the humid tropics, conversion from forest to agricultural and pastoral land use has been shown to alter vadose zone hydrology by reducing the storage capacities, infiltration rates, and lateral flow rates of forest soils [14,18–23]. For example, in the central highlands of Costa Rica, Toohey et al. [23] recorded saturated hydraulic conductivity rates in pasture and sugar cane plots of less than half the values in forested plots. Spaans et al. [22] found a twentyfold drop in saturated hydraulic conductivity in Costa Rican soils altered by pastoral land use. Studies in the humid tropics have also shown large streamflow effects after the conversion from forest to pasture (see [14]). Germer et al. [19] documented a doubling in overland flow event frequency in pasture relative to forest accompanied by a 17-fold increase in streamflow magnitude through pasture in southwestern Amazonia. Similarly, Costa et al. [24] found that mean annual discharge and peak flow increased in response to dramatic changes in land cover in southern Amazonia. Yet, the relative impacts of land use expansion and climate change on watershed-scale soil hydrology in the humid tropics remain to be discretely distinguished and quantified [3].



Figure 1. (a) Forested and (b) deforested hillslopes in the study watersheds. Observed overland flow from (c,d) sugar cane fields and (e) road surfaces (f) draining into the stream network.

Lack of long-term, high-quality monitoring data has complicated hydrological analyses aimed at evaluating the influence of land use on streamflow regimes in the tropics [3,14]. In the absence of long-term streamflow data, physically based hydrologic modeling can help quantify how increasingly intense precipitation events, rising temperatures and the prevalence of altered land cover might impact watershed and associated stream hydrology. Furthermore, in ungauged basins, there is a growing need to replace conceptual models that require calibration (e.g., Precipitation-Runoff Modeling System, Sacramento Soil Moisture Accounting Model) with models that rely on the fundamental physical processes driving the transport of precipitation through watersheds [2,3,25]. Global physical hydrology models (e.g., WaterWorld [26]) that simulate the water balance under climate and land cover change scenarios for data-poor regions with 1 ha to 1 km² spatial and monthly to annual temporal resolutions are appropriate to provide policy support for regional basins larger than the montane watersheds of the humid tropics. However, such global models rely on a simplified water balance calculation and do not simulate subsurface flow paths, soil water storage or streamflow dynamics. Furthermore, due to a lack of global datasets of subsurface parameters and an emphasis on national-scale water balance simulation, these models are not designed for daily streamflow or low-flow simulation that requires modeling soil and groundwater reservoirs. In humid tropics with deep hydrologically connected soils and limited observed data, a model is needed that can simulate daily surface and subsurface flow at a watershed scale without relying heavily on calibration. Thus, here we aim to enhance, evaluate, and employ a watershed hydrology model that can simulate existing surface and subsurface conditions for the humid tropics, but also simulate variable LUCC and climate conditions due the physically based nature of the model.

In this study, our overall goal is to determine to what degree climate and LUCC affect stream discharge at the catchment scale in humid tropical mountain watersheds, achieved via the following objectives:

1. Apply the process-based, spatially distributed Soil Moisture Routing Model (SMR) [27–31] to three watersheds in the central highlands of Costa Rica.
2. Perform a global sensitivity analysis to assess which parameters produced the largest uncertainty in model simulations using a one-cell version of the SMR model.
3. Evaluate the effects of predicted climate regime changes and land use on stream hydrology by modeling scenarios representing a matrix of climate and land use conditions in the three study watersheds.

We discuss our results in relation to the effects of land use practices on the resilience of watersheds to provide for and protect downstream communities facing climate change. Our efforts offer a rapid and inexpensive procedure for hydrological analyses without need for long-term or spatially exhaustive datasets [2,32]. The resultant model allows land managers and researchers to simulate the hydrological effects of proposed or predicted land use changes under a changing climate.

2. Materials and Methods

2.1. Study Watersheds

Three steep (river gradient > 0.002) mountain watersheds in central Costa Rica comprised the study region: the Gato, Atirro, and Platanillo (Figure 2). These study watersheds (United States Geological Survey Hydrologic Unit Code (HUC) level 3–3000 ha) are located in the Talamanca Mountains, drain to the Atlantic Ocean, and have similar area, shape, elevation gradient, average channel slope, climate, geology, and proximity to one another (Table 1 and Figure 2). The Gato watershed is covered by 99.9% primary and secondary forest with no known roads and is located within a forest reserve. Atirro has 2.5% non-forest land cover including roads within and adjacent to riparian zones. Platanillo is intensely modified with 41% of the watershed experiencing modified land cover including agriculture, pasture, and urban uses [33] (Figure 2). The land use in all three watersheds has been consistent for decades [33].

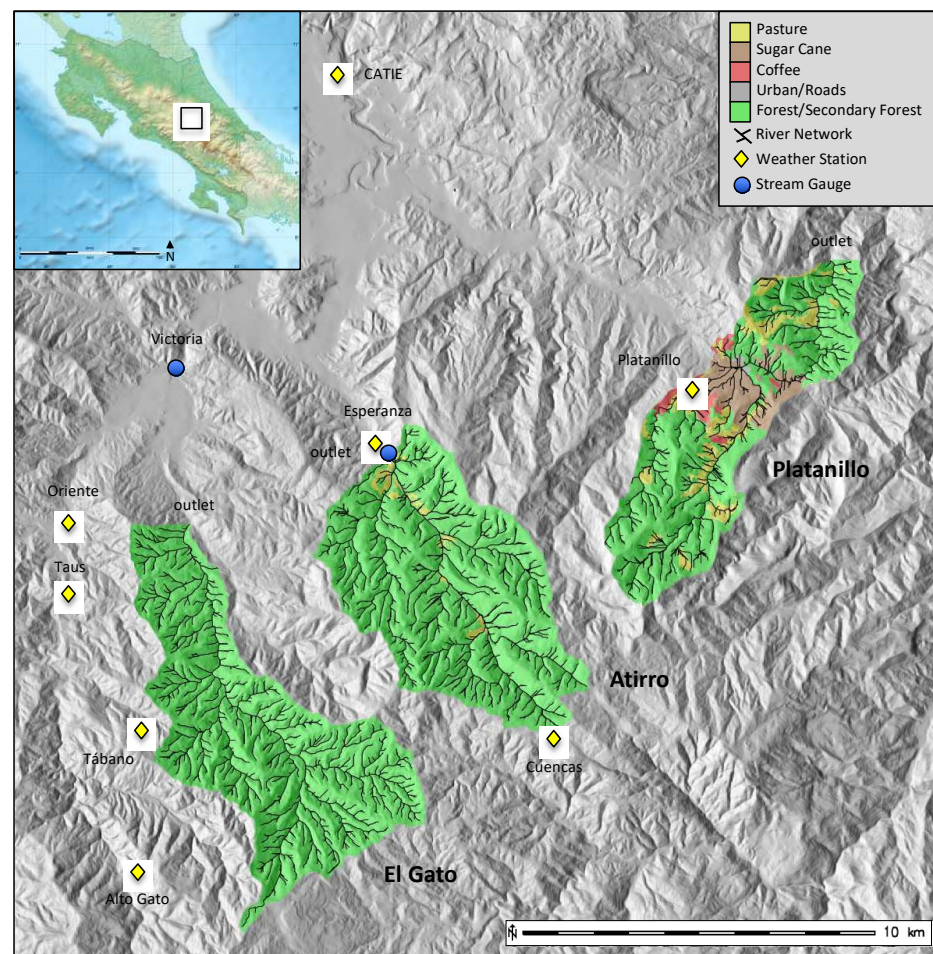


Figure 2. Location of the three study watersheds in the Talamancas Mountains of central Costa Rica showing land use distribution and the location of meteorological stations in the study region relative to the study watersheds.

Table 1. Watershed Characteristics.

Watershed	Drainage Area	Elevation Range	Max Slope	Median Slope	Altered Land Cover
Gato	3340 ha	755–2355 m	58°	31°	<0.1%
Atirro	3249 ha	780–1980 m	60°	26°	2.50%
Platanillo	2595 ha	700–1940 m	56°	24°	41.00%

The central Costa Rican highlands are characterized by frequent intense precipitation events [34,35] and deep well-developed soils [36]. The study region receives an annual rainfall average of 5250 mm (Instituto Costarricense de Electricidad (ICE)). A precipitation gradient, evident in records from meteorological stations in and near Gato and Atirro watersheds, ranges from 4620 mm at 873 m elevation to 7070 mm at 1700 m elevation. Although rain is frequent at higher elevations throughout the year, a drier season reduces precipitation during the months of February through April. A weaker gradient from west to east is also evident from the decline in precipitation between stations at similar elevation including the Alto Gato and Cuencas stations and La Esperanza and Platanillo stations (Figure 2). Soils in the region are mapped as Typic Haplohumults and Typic Dystrudepts depending on proximity to lowland alluvial valleys where Inceptisols are most common [36]. In the study watersheds, clay-rich Ultisols dominate, although soil depth varies depending on slope [37–40]. Geology and native vegetation composition are similar for all three watersheds.

2.2. Soil Moisture Routing Model

We simulated watershed hydrology using the process-based, spatially distributed Soil Moisture Routing (SMR) model. Appropriate for both deep and shallow soils, SMR simulates surface and subsurface watershed flow paths and streamflow (Figure 3). The SMR model does not rely on calibration of the dominant processes (i.e., soil–water relationships, lateral flow), and thus is suitable to determine if changes in land use could offset predicted climate-driven changes in precipitation and temperature. The model’s design allows the user to spatially represent watershed vegetation, soil conditions, precipitation and temperature, and hence provides full control to develop specific land use and climate scenarios. The SMR model is GIS-based and parameterization requires a relatively low amount of observed data, demonstrating its potential as an application in data-poor regions of the world, particularly where subsurface flow paths are critical for accurately simulating streamflow at time scales shorter than one month and at spatial scales greater than a 1 ha resolution.

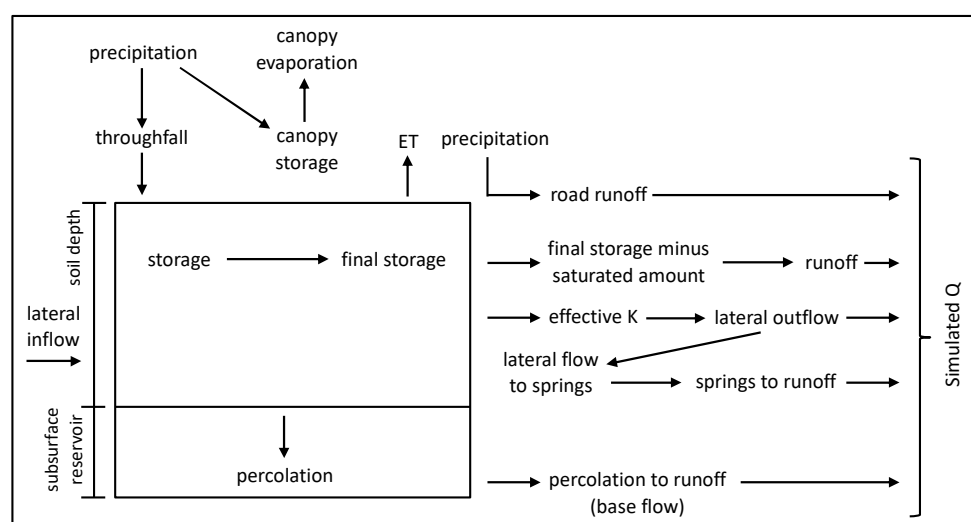


Figure 3. Primary inputs, outputs, and flow pathway interactions for each cell in the SMR model. The flow rates for each pathway are spatially represented as individual raster maps in the model setup, and thus the model can simulate rate variability across a watershed. For each time step, SMR adds the amount of precipitation and lateral inflow from neighboring upslope cells before calculating the amount moving along each flow path. Soil water not retained in storage exits each cell as evapotranspiration, deep percolation, lateral throughflow, and runoff. Lateral outflow adds to the storage of downslope cells unless it intersects a channel, becoming spring runoff. Runoff also occurs where infiltration capacity is restricted (e.g., road runoff) or the cell’s final storage value surpasses its saturation amount. The contribution of subsurface reservoir water to runoff depends on the subsurface storage amount at a given time step and the reservoir’s recession coefficient(s). All runoff is added to the simulated watershed discharge at the end of each time step.

We ran the SMR model script in the open-source GIS software GRASS v.7.8 (Geographic Resource Analysis Support System, <http://grass.osgeo.org/>). Each parameter in the model is represented by a single raster with 10 m cell size (Table 2). Layering spatial data that represent soil parameters in the GIS environment allows the model to calculate the water balance for each cell at each time step (Figure 3). The model simulates the timing and magnitude of flow at the watershed outlet to generate hydrographs aligned to the time step set in the model. We assigned daily time steps to model runs based on the daily resolution of available precipitation and temperature data, although we also ran the model at a two-hour time step by dividing daily precipitation totals to estimate different rainfall intensities and simulate higher resolution hydrographs.

Table 2. Input Parameters for Soil Moisture Routing Model.

SMR Input Parameter	Source	Value
Precipitation (not in GSA)	Meteorological station data (ICE), Climate models [7,8]	See Figure 4
PET (not in GSA)	Hamon PET equation	Calculated ET: 0.16–0.24 cm/day
Crop Coefficient	General value for humid tropical vegetation [41]	0.8
Soil Depth	Field sampled and corrected for slope; depth of hydrologic soil layers A and B adopted from [20,23]	Forest: A: 35 cm, B: 65 cm Coffee: A: 50 cm, B: 50 cm Sugar Cane: A: 50 cm, B: 50 cm Pasture: A: 10 cm, B: 90 cm Road †: A: 50 cm, B: 50 cm
Slope (not in GSA)	DEM	Range: 0–62° Forest: A: 13.4, B: 8.9 cm/day Coffee: A: 7.7, B: 8.9 cm/day
K_{sat} Matrix	[20,22,23]	Sugar Cane: A: 3.1, B: 1.7 cm/day Pasture: A: 2.9, B: 5.5 cm/day Road †: A: 0.05, B: 0.05 cm/day Forest: A: 134.4, B: 88.8 cm/day Coffee: A: 76.8, B: 88.8 cm/day
K_{sat} Macropore	[20,22,23]	Sugar Cane: A: 31.2, B: 16.8 cm/day Pasture: A: 28.8, B: 55.2 cm/day Road †: A: 1.0, B: 1.0 cm/day Forest: 84.0 cm/day Coffee: 84.0 cm/day
K_{sub}	[23], Estimated	Sugar Cane: 1.4 cm/day Pasture: 4.8 cm/day Road †: 1.4 cm/day Forest: 28% Coffee: 28%
Field Capacity Moisture Content	[23]	Sugar Cane: 28% Pasture: 18% Road †: 8% Forest: A: 38%, B: 28% Coffee: A: 38%, B: 28%
Porosity (Saturated Moisture Content)	Field sampled; [22]	Sugar Cane: A: 38%, B: 28% Pasture: A: 28%, B: 18% Road †: A: 3.8%, B: 2.8%
Residual Moisture Content	[22,23]	All land cover types: 2%
Wilting Point Moisture Content	[23]	All land cover types: A: 1.94%, B: 1.21% Forest: 0.2 cm Coffee: 0.1 cm
Max Canopy Storage Amount (not in GSA)	[42]; Estimated	Sugar Cane: 0.05 cm Pasture: 0.05 cm Road: 0.0 cm
Rock Content	Field sampled	All land cover types: 10% Atirro: 7.66 ha; 0.24% cover
Road Area (not in GSA)	[32], Aerial imagery	Gato: 0 ha; 0% cover Platanillo: 22.98 ha; 0.89% cover
Recession Constants (not in GSA)	Estimated based on gauge data	a = 75; b = 0.2 (See equation in text)
Antecedent Moisture Content (not in GSA)	Estimated (model equilibrates)	72 cm

GSA—Global Sensitivity Analysis; upper (A) and lower (B) soil layers; † all road parameters estimated.

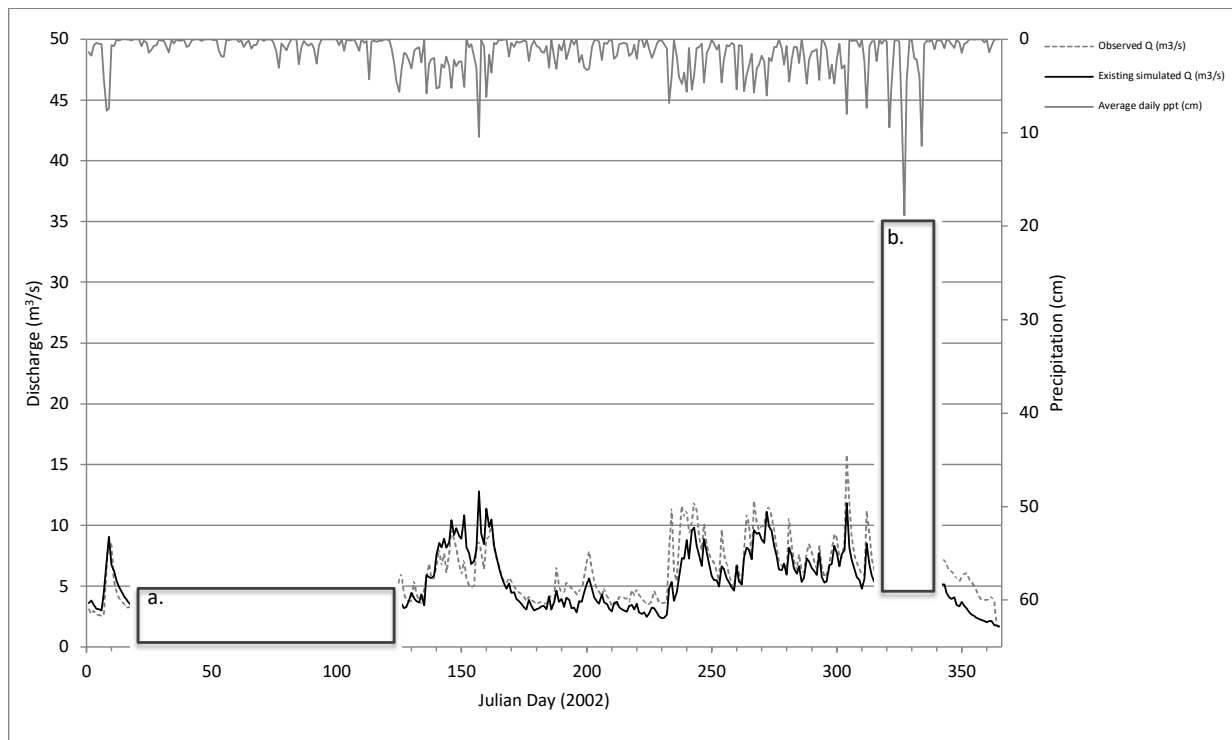


Figure 4. The observed and simulated Atirro daily-time step hydrographs plotted with daily precipitation. “Existing” refers to the land use scenario used in the watershed simulation. $N_s = 0.73$. Box (a) highlights the model’s limitation in simulating baseflow during the dry season. Box (b) highlights the model’s deficiency simulating short duration peak flow events. No calibration was applied.

We chose SMR parameter estimates (Table 2) based on plot-scale measurements of soil parameters from published regional studies, field-measured soil properties from our three study watersheds, and one year of local meteorological station data (Tropical Agricultural Research and Higher Education Center—CATIE, Instituto Costarricense de Electricidad—ICE). Spaans et al. [22], Hanson et al. [20], and Toohey et al. [23] reported soil hydrology parameters from plot-scale soil hydrological analyses of land use effects under topographic, soil and climate conditions similar to our three study watersheds described above (forest, coffee, sugar cane, and pasture) and all distinguished the importance of macropore flow. The Ultisol soils described in Hanson et al. [20] and Spaans et al. [22] most closely agree with the soil type mapped in the three study watersheds [36]. While the soils described in Toohey et al. [23] are in closer proximity to our watersheds, their andic properties represent more porous soils than clay-rich Ultisols exhibit. Thus, we selected conservative soil parameter values based on these regional studies coupled with field-based observations from our study watersheds in place of an intensive soil survey. Specifically, we assigned matrix and macropore saturated hydraulic conductivity values (K_{sat}) and subsurface hydraulic conductivity values (K_{sub}) from the more comprehensive soil hydrology measurements reported by Toohey et al. [23] while adopting porosity values based on Spaans et al. [22] and our own soil samples. However, given the andic properties of the Toohey et al. [23] soils, we also separately simulated the hydrologically restrictive soil layer in pasture plots described by Spaans et al. [22] and Hanson et al. [20] by lowering macropore (A: 1.0 cm/day; B: 6.0 cm/day, where A represents upper and B represents lower soil layers) and subsurface (1.0 cm/day) hydraulic conductivity values.

Deep reservoir behavior represents the most difficult flow path to model without extensive hydrogeologic surveys [43,44]. Thus, linear and nonlinear recession equations are generally used to estimate groundwater contribution to streamflow, and these mathematical solutions remain the standard means for aligning simulated baseflow contribution to observed hydrographic trends [45]. Fortunately, the recession constants, derived from

existing stream gauge data where available, required no hydrogeological sampling to constrain realistic values, and were adjusted to closely match the falling limb of observed hydrograph data. In addition, the antecedent storage parameter (initial soil water storage amount set in the model) equilibrated within the first months of a simulation, preventing need for calibration. Typically, the antecedent storage amount is best set when there are either clearly dry conditions or clearly wet conditions. We chose relatively wet conditions given the streamflow values at the start of the modeled year. The SMR model accumulates deep percolation water in a groundwater storage reservoir which is updated after each time step. We simulated baseflow (Q_b) from this storage reservoir in the three watersheds using a nonlinear reservoir equation and derived the recession constants from the observed recession curves in stream gauge data from Atirro and Gato watersheds (sensu [45]):

$$Q_b = \left(\frac{P_c}{a} \right)^{\left(\frac{1}{b} \right)}$$

where P_c is the cumulative deep percolation at each time step, and a and b are recession constants.

2.3. Model Performance Assessment

We assessed model accuracy using the Nash–Sutcliffe efficiency parameter (Ns) by comparing model output hydrographs with the discharge record available from the gauged Atirro watershed [46]. A Ns value of 1.0 represents perfect agreement between simulated and observed data, whereas a Ns of 0.0 indicates that the model simulations are no better than the mean of observed data. According to Moriasi et al. [47], Ns value greater than 0.50 is considered ‘good’ and satisfactory for watershed streamflow models. For uncalibrated models, an Ns below 0.2 is considered inadequate, 0.2–0.4 sufficient, 0.4–0.6 good, 0.6–0.8 very good, and greater than 0.8 excellent [48]. To validate the model results for the ungauged Gato watershed where direct comparison to actual stream discharge values was not possible, we first determined the proportion of flow contributed by the Gato subwatershed within the larger gauged Pejibaye watershed. We then compared simulated Gato discharge values to the proportion of observed discharge at the Pejibaye gauge record contributed by the Gato watershed to assess model accuracy using the Ns parameter. No gauge data exist for Platanillo, and thus we justified the results based on the success of the model simulations from neighboring Atirro and Gato. We also assessed model performance using the root mean squared error, mean absolute error and R-squared values comparing observed watershed discharge values to simulated values (see [28]).

The performance criteria, based on a one-year model run compared with observed data, provide model validation. This validation justifies use of scenarios representing different land cover and climate conditions. Calibration was not performed because SMR is a physically based model—a main benefit of using physically based models is reduced reliance on calibration. Non-physically based models can only function if calibrated, which limits model applications only to those watersheds where large, long-term data exist. Our model parameter values were chosen based on measurements in the area where the model was applied (see [49]).

2.4. Model Sensitivity Analysis

Sensitivity analyses help determine which parameters most strongly influence model predictions and aid accurate parameterization of hydrological models. We evaluated the sensitivity of the SMR model parameters in humid tropical watersheds using modeling results from a one-cell version of the Atirro watershed model. While the one-cell model does not spatially distribute parameters, the analysis does evaluate the sensitivity of model parameters based on the widest theoretical range of each parameter’s variance. To perform this assessment, we upscaled the plot-scale observations of soil hydrology parameters to the watershed scale, linking first-order hillslope processes to streamflow dynamics

through the known hydrological pathways illustrated in Figure 3. We then assessed the sensitivity of the SMR model parameter estimates (Table 2) using the global sensitivity analysis (GSA) approach described by Harper et al. [50]. This approach uses Random Forest [51] to calculate Gini Importance values for individual parameters based on how an individual decision tree influences the error rate. The Gini Importance value estimates the change in model output (i.e., watershed discharge) created by comparing different model runs and gives a cumulative importance per parameter across the permuted decision trees. This approach in the sensitivity analysis accounts for interactions among parameter estimates that influence the calculated output, which is important in complex simulation models [50].

We tested parameter importance with the widest possible theoretical parameter space for five different hydrological response variables: annual minimum flow (set at a threshold of 1.6 m³/s), annual peak flow (set at a threshold of 30 m³/s), peak flow duration, low flow duration, and standard deviation in wet season flow (days 125–339 of modeled year 2002). First, we designated three estimates for each parameter within the theoretical range of each of the 12 model parameters for the humid tropics. Second, we randomly selected 5000 sets of parameter estimates for a one-year, single-cell model of the Atirro watershed. We used the 2002 Esperanza gauge (Figure 2) record for the input precipitation. Third, we ran 5000 one-year iterations of the one-cell SMR model using these parameter estimates and recorded the five response variables from the simulations. The parameter estimates and the five hydrological response outputs were put into a matrix and analyzed using Random Forest (RandomForest; R Foundation for Statistical Computing Platform, 2015). We normalized the Gini Importance values to show the relative importance of each hydrograph parameter.

2.5. Climate Scenarios and Land Use

We created a matrix of input model parameter estimates that represent current and future climate and land use scenarios in the three watersheds to test the effects of land use and climate on streamflow independently and jointly (Tables 2 and 3). Climate scenarios represent changes in precipitation and temperature regime, and land use scenarios represent changes in soil conditions associated with vegetation cover.

Table 3. Two-Hour Time Step Simulation Scenario Matrix.

Watershed	Land Use	Rainfall Intensity	Temperature (Based on 2002 Record)	Rainfall Amount (% of 2002 Precipitation)
Atirro	All pasture	High rate	Existing Temperature	70%
	Existing	Existing rate	+1 °C (daily time step only) +4 °C	100% 110%
Gato	All pasture	High rate		
	Existing	Existing rate		
Platanillo	All pasture	High rate		
	Existing	Existing rate		
	All forested	Existing rate		

To simulate predicted climate change, we modeled three rainfall intensities in all three watersheds at two-hour time steps (Table 3) based on regional IPCC climate predictions [6]. To simulate changes in rainfall intensity, we first calculated “existing” precipitation intensity by taking the 2002 gauged daily precipitation total and distributing it over 24 h. Then, we concentrated the rainfall total to a 16-h period of evenly distributed precipitation bound by four hours at half the intensity before and after the central 16-h period. Next, we calculated the “high” rainfall intensity rate by reducing the duration of the 24-h daily rainfall distribution to six hours with the median two-hours receiving the highest intensity. In addition to simulating rainfall intensities, we altered total rainfall amounts to represent 70%, 100%, and 110% of measured precipitation in the Atirro watershed recorded at the Esperanza and Cuencas rain gauges from 2002 (Table 3 and Figure 2). We also simulated

temperature change for the Atirro watershed by modeling the recorded 2002 temperatures and an extreme 4 °C temperature increase above the 2002 record for each land use and rainfall scenario at a two-hour resolution. We added a 1 °C temperature increase to scenarios at a daily resolution; however, we focus our results on the two-hour resolution simulations. The model then derives potential evapotranspiration loss for each time step from the input temperature through the addition of the Hamon [52] equation to previous published iterations of SMR:

$$PET = k \times 0.165 \times 216.7 \times N \times \frac{e^s}{T + 273.3}$$

where k is the proportionality coefficient, N is daytime length ($\times/12$ h), e^s is saturation vapor pressure (mb), and T is average daily temperature (°C). Actual evapotranspiration is then calculated as PET for each time step multiplied by the ET crop coefficient and each cell's moisture content as in Brooks et al. [28].

To simulate LUCC, we created two land cover change scenarios in the three study watersheds defined by different vegetation and associated soil parameters (Table 2). These scenarios represent existing land cover and complete pasture conversion (Table 3). While the existing Gato watershed is 100% forested, the existing Atirro land use scenario represents the present day 2.5% deforested land cover—primarily riparian forest converted to pasture, sugar cane and roads—with the remaining 97.5% forested. The existing Platanillo watershed is a mixed matrix of land cover representing 41% altered land cover and 59% forested, providing an example of partial forest conversion (Figure 2 and Table 1). Consequently, we created a third completely forested scenario for the Platanillo watershed given its greater deforested proportion relative to the other two dominantly forested watersheds. All three watersheds were modeled in their existing land cover state and in a complete pasture conversion state while retaining any existing urban areas and road networks at two-hour and daily temporal resolutions. We then evaluated how each modeled scenario (Table 3) influenced watershed hydrology by comparing simulated output hydrographs for the Atirro and Gato watersheds to the observed hydrographs from the simulated year. For the Plantanillo watershed, we were only able to evaluate relative differences among the simulated hydrographs for the three land cover scenarios under different rainfall intensities since no gauge data existed for this watershed.

To analyze the integrated effects of climate change and LUCC on watershed hydrology, we simulated one-year scenarios of precipitation, temperature, and land use combinations at both daily and two-hour temporal resolutions (Table 3) in the Atirro watershed. The scenario matrix combined rainfall amount (70%, 100%, and 110% of the 2002 daily amounts) and intensity variations (high: daily rainfall condensed to six hours; low: daily rainfall spread across 24 h) with temperature variations (+0 °C, +4 °C at a two-hour resolution and +0 °C, +1 °C, and +4 °C at a daily resolution derived from the observed 2002 average daily temperatures) for the two Atirro land cover scenarios described above. This matrix generated 24 simulations of climate and land use combinations at a two-hour resolution. Among all 24 scenarios, we compared modeled streamflow trends, including peak and low flow events and peak and low flow duration. Our primary assessment of climate versus LUCC relied on comparing the summed 24 top peak discharges from each two-hour time step simulation since peak flows represent primary hydrological and geomorphic drivers of change in river systems. We also analyzed the simulated mass balance at a daily resolution to identify which modeled surface and subsurface flow paths (i.e., evapotranspiration, baseflow, runoff, and storage) changed in response to LUCC.

3. Results

3.1. Model Performance

The SMR model performance was 'very good' with an N_s value of 0.73 for the Atirro gauge and a value of 0.65 for the 56% portion of the Pejibaye River discharge representing the Gato watershed contribution. Multi-day wet periods and troughs between peak flow

events were modeled very well (Figure 4), while the model slightly underestimated both baseflow (40–45%; Figure 4a) and peak flows relative to observed values (10–40%). Two of the largest peak flows represent the greatest underestimated model differences with the observed data (Figure 4b) and thus disproportionately contribute to the root mean squared errors of 1.90 m³/s for Atirro and 2.67 m³/s for Gato. The mean absolute error indicates an average daily discharge prediction error of 0.92 m³/s for Atirro and 1.49 m³/s for Gato. The r² value of simulated to gauge data is 0.79 for Atirro and 0.66 for Gato.

3.2. Sensitivity Analysis

The one-cell model parameter sensitivity analysis of the Atirro watershed shows that the response variables (Peak Flow, Peak Duration, Low Flow, Low Duration, Wet Season Standard Deviation) are most sensitive to variation in macropore K_{sat} , soil depth, porosity, and K_{sub} (Table 4). Rock content, residual moisture content, and field capacity moisture content minimally influenced the response variables (4–10%). Maximum canopy storage, wilting point moisture content, and soil matrix K_{sat} did not strongly influence any of the five response variables (<4%).

Table 4. Gini Importance Values in SMR Sensitivity Analysis.

	LowDuration	PeakFlow	PeakDuration	WetStandDev		
Field Capacity Moisture Content	3.7%	8.9%	6.2%	4.4%	5.8%	
Subsurface K	2.9%	4.0%	23.7%	3.1%	14.2%	
Macropore Ksat	45.4%	25.9%	19.9%	27.5%	42.0%	
Matrix Ksat	2.7%	3.7%	3.6%	3.1%	3.3%	
Max Canopy Storage	2.8%	3.8%	3.7%	3.1%	3.2%	
Porosity	14.3%	12.8%	15.8%	15.1%	9.8%	
Residual Moisture Content	5.7%	8.3%	5.0%	6.3%	4.8%	
Rock Content	7.3%	9.8%	6.6%	8.4%	5.4%	
Soil Depth	12.5%	19.2%	11.9%	25.9%	8.4%	
Wilting Point Moisture Content	2.7%	3.6%	3.6%	3.2%	3.2%	
Scale	0.0%	10.0%	20.0%	30.0%	40.0%	50.0%

3.3. Land Use and Climate Scenarios

3.3.1. Land Use Effects

In all three watersheds, the effects of LUCC, and thus altered hydrological flow paths, are evident in the simulated hydrographs that show significant peak flow increases (65–85% higher) and event duration decreases (Figure 5), particularly if a hydraulically restrictive layer (i.e., weakly permeable soil layer) exists (Figure 6). The results of Plantanillo watershed simulations representing the existing mixed land cover (partial forest conversion; 41% converted) and complete forest conversion demonstrate trends of high flow spikes and subsequent rapid drops relative to the simulated fully forested Platanillo watershed, a scenario like the existing forested land cover scenarios for Atirro and Gato (Figure 5c). The shorter two-hour time step produced peak flows in Atirro that fluctuated more drastically for the pasture-dominated land use scenarios than seen in the simulated daily average hydrographs (Figure 5d). Simulation of a hydraulically restrictive soil layer in the pasture conversion scenario for Atirro indicates a substantial effect on baseflow signified by rapid discharge drops below observed baseflow levels following amplified peak flow events (Figure 6). Increasing precipitation intensity did not strongly alter average daily discharge in simulations of forested watersheds, whereas in the pasture conversion scenarios it generally caused increased daily peak flows (Figure 7). The two-hour time step simulations of increased rainfall intensity coupled with land use scenarios provided greater temporal resolution for distinguishing the relative influences of climate and LUCC (Figure 7c).

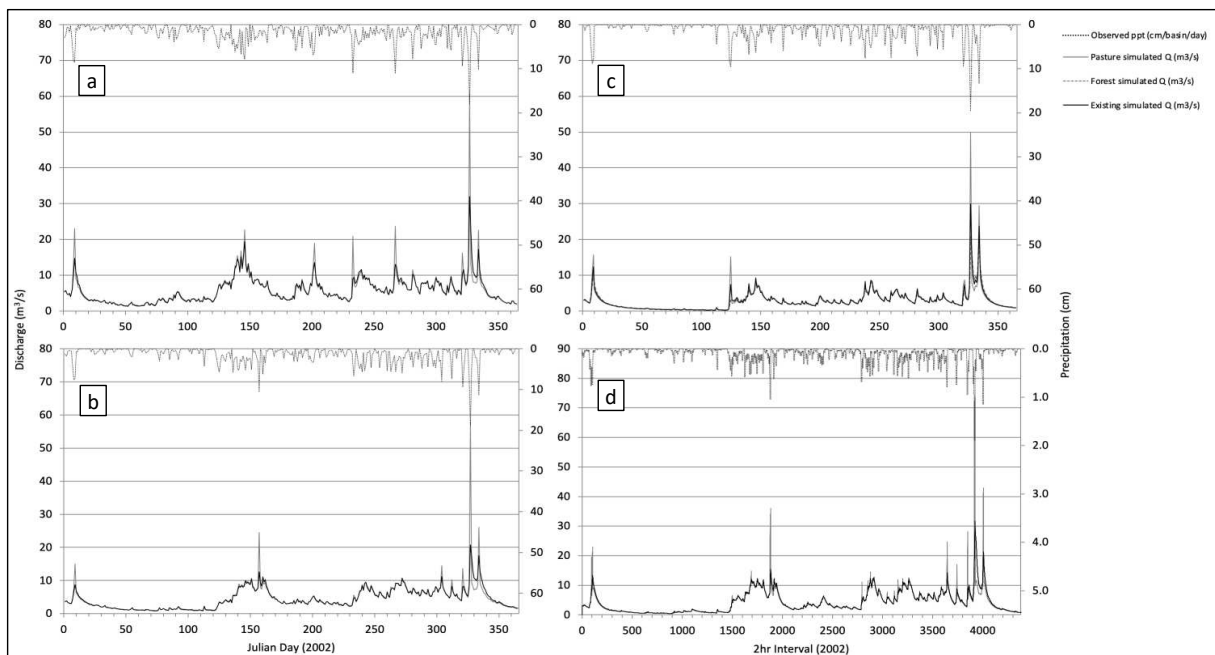


Figure 5. Hydrographs representing simulated land use conversion versus existing land cover using the 2002 precipitation record for the three study watersheds (a) Gato, (b) Atirro, (c) Platanillo, and (d) Atirro two-hour time step. (a) Gato simulated daily discharge for existing and all-pasture land use scenarios. (b) Atirro simulated daily discharge for the existing and all-pasture land use scenarios. (c) Platanillo simulated daily discharge for existing, all-forest and all-pasture land use scenarios. (d) Atirro simulated discharge for the existing and all-pasture land use scenarios at a two-hour interval. Note the greater peak flow magnitudes and more rapid drop following large peak flows in pasture relative to forested simulations.

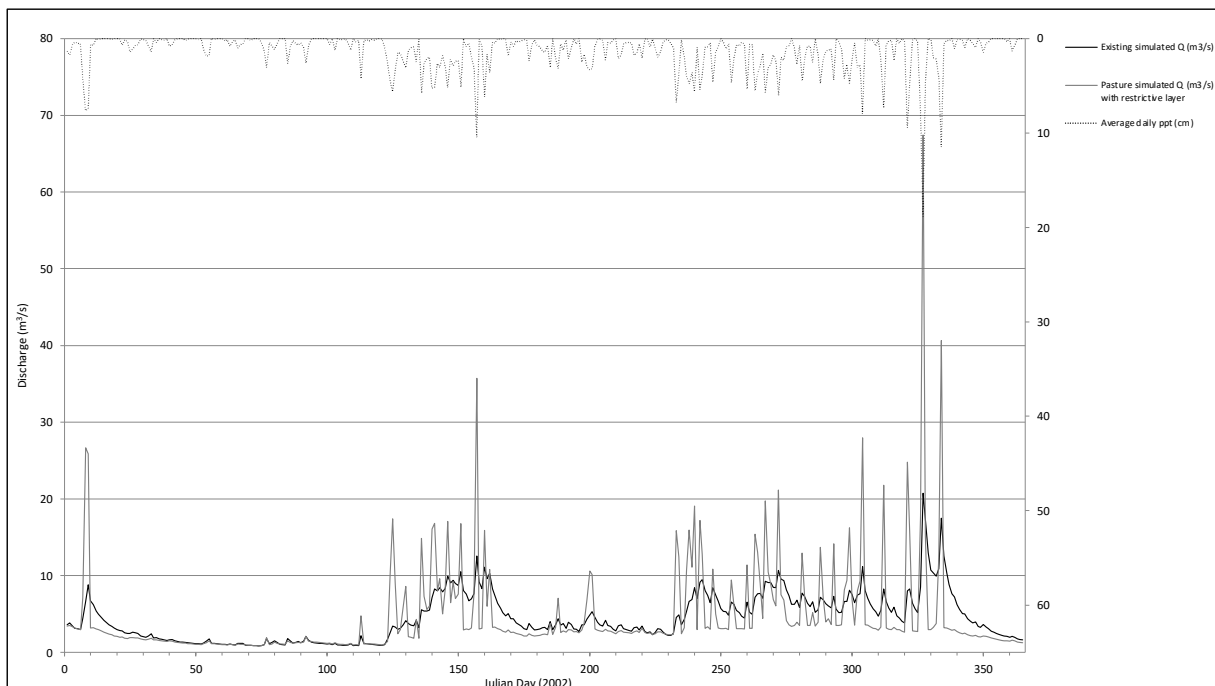


Figure 6. Daily resolution hydrographs showing the effect of simulating a restrictive layer at 10 cm below the surface in the pasture conversion scenario in Atirro. Note the rapid drop to a lower baseflow level relative to the existing land cover scenario following amplified peak flow events.

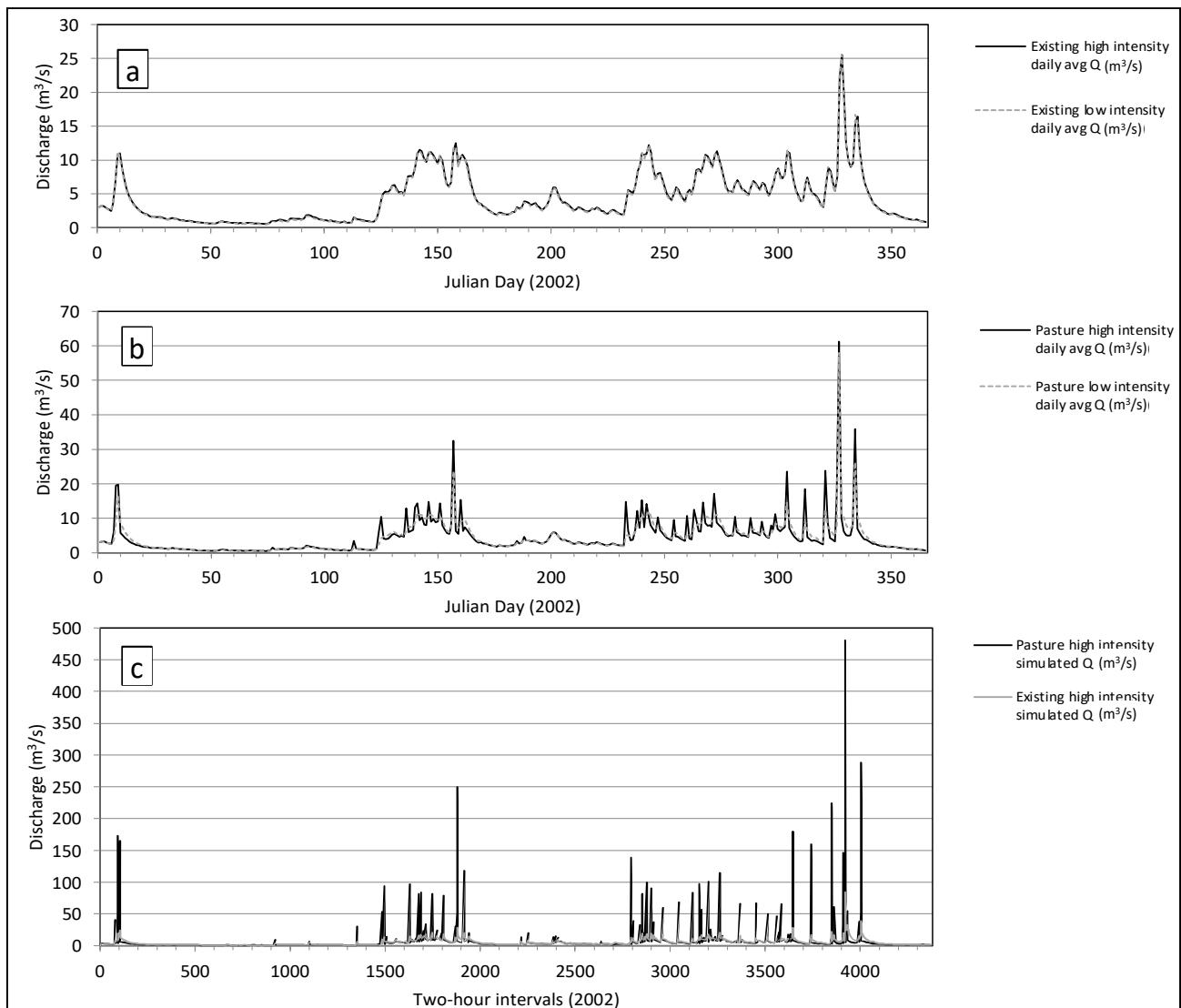


Figure 7. Hydrographs representing low and high precipitation intensity on existing land cover and pasture conversion scenarios in Atirro. The effect of precipitation intensity was estimated using (a) daily discharge values averaged from 2 h time step simulations and the existing land cover, (b) daily discharge averages and all-pasture conversion, and (c) 2 h time step in existing and all-pasture land cover.

3.3.2. Combined Climate and Land Use Effects

A more detailed comparison of the modeled Atirro watershed responses to combined land use and precipitation scenarios indicates a stronger effect of altered precipitation intensity and amount on forest converted to pasture than intact forest while temperature increases weakly influence discharge values via modeled *ET* (Figures 7–9). The sum of the 24 largest simulated discharge values is greater across all climate scenarios an average of 1427 m³/s in pasture compared to forest land cover, ranging from an increase of 211 to 3230 m³/s depending on the climate scenario. In particular, high precipitation intensity raises the sum of top peak flow events an average of 94 m³/s and 2094 m³/s in forest and pasture scenarios, respectively. At 70%, 100%, and 110% of measured precipitation, the summed top-24 discharge values for forested scenarios under both low and high intensity are similar, showing differences of 13–16%: 344 vs. 396 m³/s, 605 vs. 704 m³/s, and 699 vs. 832 m³/s, respectively (Figure 9). However, the summed top-24 discharge values representing pasture scenarios diverge significantly between the low and high precipitation intensities. While the summed discharge values of all low precipitation

intensity scenarios positively correlate with increased precipitation amount, the high-intensity pasture scenario tripled the summed discharge value for all three precipitation amounts: 70%—560 to 1737 m³/s; 100%—1107 to 3486 m³/s; and 110%—1263 to 4063 m³/s. In contrast, extreme temperature increases of +4 °C only minorly impacted the peak discharge values through changes to *ET* loss, although slightly more discharge is lost to *ET* in pasture scenarios than forested (Figures 8 and 9). Temperature increases of 4 °C decrease the summed 24 top discharges an average of 12.6 m³/s via *ET* loss in forested land cover scenarios and 38.0 m³/s in pasture scenarios. Daily-resolution simulations of the existing forested Atirro watershed display increases in *ET* losses of 8.4% (5.0 cm/basin/yr) and 36.4% (21.0 cm/basin/yr) with +1 °C and +4 °C temperature increases, respectively, from the measured 2002 precipitation total of 504 cm. Two-hour-resolution simulations of forested and pasture conditions in Atirro with a +4 °C increase resulted in *ET* losses of 30.6% (20.8 cm/basin/yr) and 30.0% (21.0 cm/basin/yr) greater, respectively, than losses simulated with actual 2002 temperatures.

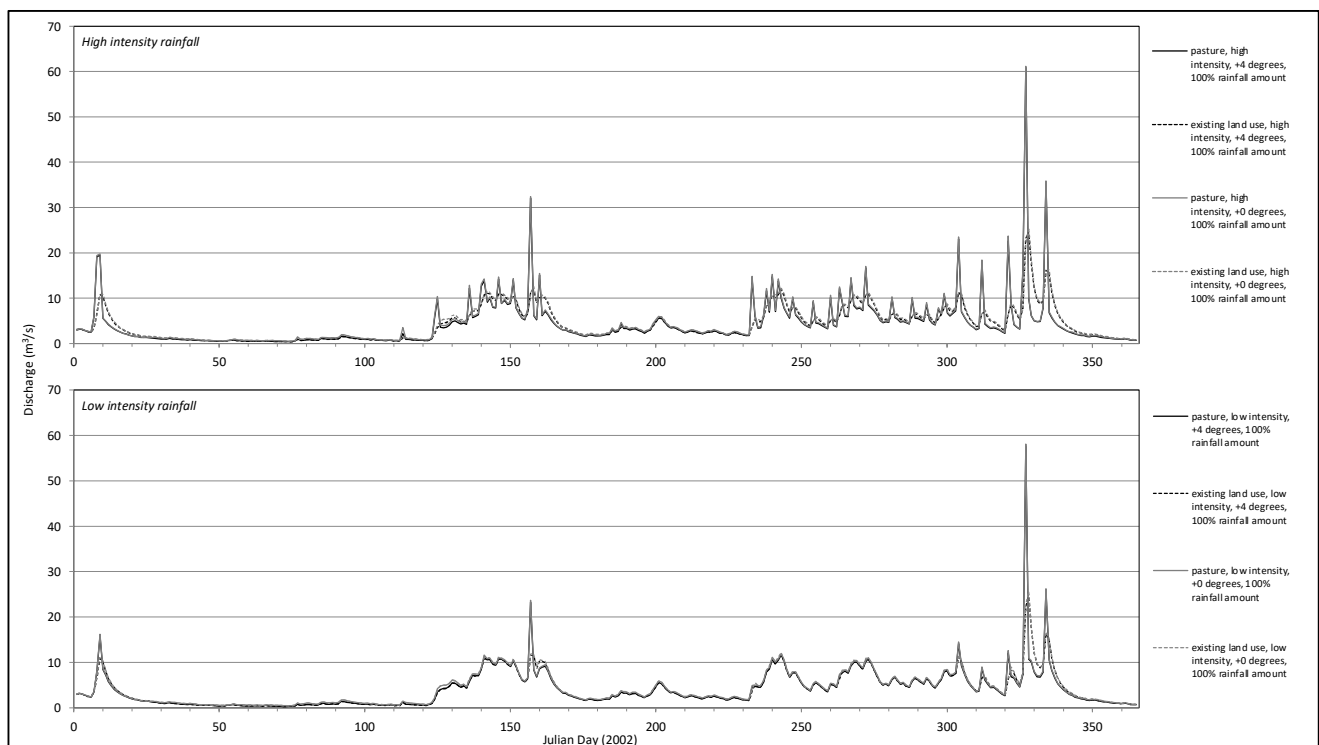


Figure 8. The effect of rainfall intensity and temperature increase (via *ET*) on discharge from existing forested land cover in Atirro compared to simulated pasture conversion. Daily discharge averages are derived from averaged two-hour time step values for each day in order to express the effect of rainfall intensity. Note the overall weak effect of temperature increase on discharge relative to LUCC. Precipitation intensity and amount influence discharge more than temperature, but less than LUCC.

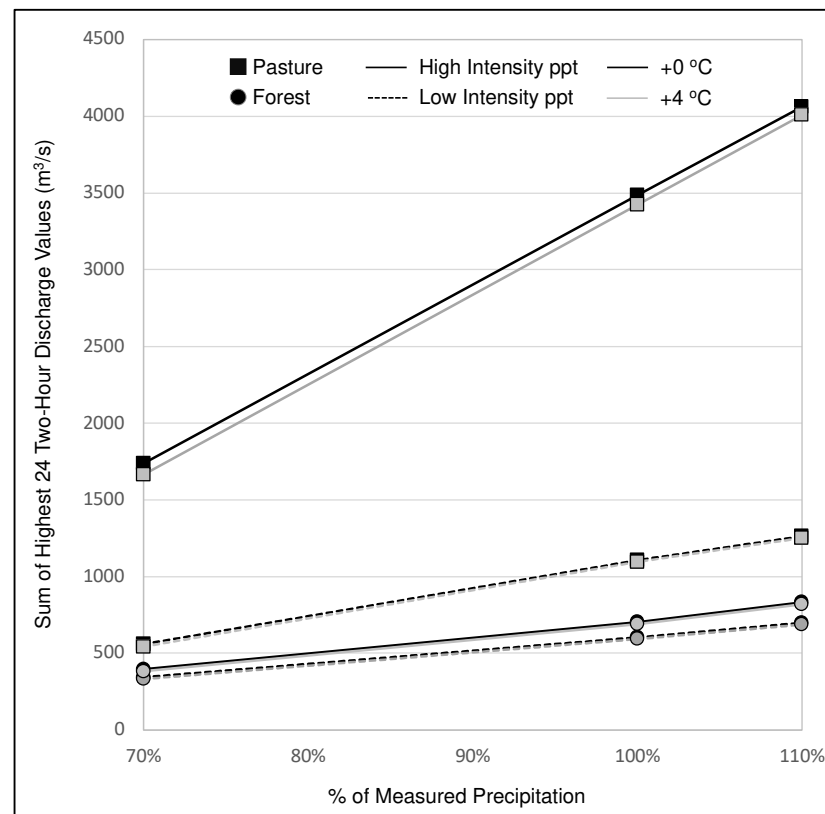


Figure 9. Influence of temperature increase and precipitation intensity and amount on the highest 24 two-hour discharge values derived from year-long simulations of Atirro watershed hydrology under existing forested and complete pasture conversion scenarios. Effects of varying precipitation intensity and amount are greater under the pasture conversion scenario than the existing forested land cover scenario. Varying precipitation makes little impact on the forested watershed hydrology whereas the pairing of higher intensity rainfall events with pasture conversion raises the sum of the 24 highest discharge events nearly an order of magnitude from the forested scenarios. The effect of increasing temperature on ET has the least influence on discharge of the simulated climate variables.

3.3.3. Land Use Effects on Flow Paths

The relative contributions of each hydrological pathway to the annual water budget derived from the mass balance for both the forested and pasture-converted Atirro watershed simulations indicate how LUCC changes flow paths (Table 5). Percolation-derived baseflow contributes 76.5% of total basin streamflow in the existing forest-dominated land cover configuration whereas overland runoff accounts for only 7.4% of the annual output. Simulated conversion to pasture using conservative matrix and macropore K_{sat} values causes an increase in runoff (37.1 cm/yr vs. 59.8 cm/yr) in place of baseflow. The reduced macropore K_{sat} and K_{sub} rates used to simulate a hydraulically restrictive layer associated with pasture LUCC increase saturation-excess runoff to 45.5% (229 cm) of the total annual water budget (Table 5 and Figure 6). Our simulation of the existing land use configuration in Atirro indicates a 4.5% storage coefficient, or the fraction of the overall water balance maintained in subsurface storage at the end of the year, relative to 1.4% storage in the pasture conversion. Storage includes water occupying soil pore space (percent saturation) and active lateral flow at the end of the simulated year. In both land cover simulations, the final water balance is slightly negative in the groundwater reservoir, indicating a net loss from the initial storage amount: 7.7 cm (~1.5%) from the existing modeled watershed and 8.0 cm (~1.6%) from the pasture-converted watershed. Simulated ET is similar for both land cover configurations at approximately 60 cm total lost per year across the basin, accounting for 12% of the water budget, a reasonable value for the humid tropics but slightly lower than [53], who measured annual actual ET of 73–79 cm directly in a nearby watershed.

Table 5. Atirro Mass Balance (Daily Time Step Simulations).

Atirro Existing			Atirro Pasture Conversion			Atirro Pasture with Restrictive Layer		
MASS BALANCE		DEFICIT	MASS BALANCE		DEFICIT	MASS BALANCE		DEFICIT
ppt input (cm/basin)	output (cm/basin)	ppt-output	ppt input (cm/basin)	output (cm/basin)	ppt-output	ppt input (cm/basin)	output (cm/basin)	ppt-output
503.5	480.8	22.7	503.5	496.3	7.2	503.5	496.3	7.2
Water Balance Term	%	cm	Water Balance Term	%	cm	Water Balance Term	%	cm
Precipitation	100.00%	503.5	Precipitation	100.00%	503.5	Precipitation	100.00%	503.5
Evapotranspiration	11.60%	58.4	Evapotranspiration	12.30%	61.8	Evapotranspiration	12.30%	61.8
Baseflow	76.50%	385.3	Baseflow	74.40%	374.8	Baseflow	40.80%	205.6
Saturation Excess	7.40%	37.1	Saturation Excess	11.90%	59.8	Saturation Excess		
Runoff			Runoff			Runoff	45.50%	229
Storage	4.50%	22.7	Storage	1.40%	7.2	Storage	1.40%	7.2

4. Discussion

Interpretation of our simulated climate and land use scenarios is contingent on model performance as a measure of its validity, and effective use of the model outside our study region depends on knowledge of the most sensitive parameters as a measure of the model's robustness [54]. Accordingly, in the following section, we first consider model performance, then interpret how model parameters influence the response variables assessed in the sensitivity analysis, explain how these results can inform modeling efforts, and discuss the model's capability to simulate observed watershed conditions. Finally, we discuss the influences of climate and LUCC on watershed hydrology.

4.1. Model Performance

SMR effectively simulates humid tropical mountain watershed hydrology for a single year of the Atirro gauge ($N_s = 0.73$; Figure 4), most accurately for troughs between peak flow events and multiday wet periods; however, the model could benefit from a more physical representation of shallow groundwater contributions to baseflow (e.g., soil macropore networks and springs) and effects of impermeable surfaces (e.g., roads) on short-duration peak flows. SMR underestimates baseflow during the dry season (40–45%; Figure 4a), possibly due to unaccounted groundwater contribution to stream discharge. Groundwater traveling along regional faults [55] may maintain the higher baseflow compared to modeled results during the dry season in the Atirro watershed. This could be further assessed with longer-term datasets in the future. The decreased accuracy of certain simulated peak flow events and baseflow periods (Figure 4a,b) are minor relative to the simulated hydrological impact we see with vegetation cover change (Figures 5–8). We report the model's limitations to supplement the 'very good' model performance metrics and highlight where the model could be improved if more were known about subsurface conditions, such as soil macropore networks and structural faults.

In addition, high temporal resolution precipitation records can improve model precision, particularly for peak flow events. Daily precipitation totals restricted precise estimation of precipitation intensity over the course of a day (Figure 4b), flattening the rapidly responsive flow peaks and troughs we observed in the field. In flashy humid tropical mountain watersheds such as Atirro, daily flow averages artificially minimized flow peaks that pass through the channels in response to intense rainfall. Heightened temporal resolution can also simulate changes in watershed response due to LUCC more precisely (Figures 5d and 7c).

4.2. Sensitivity Analysis

Results of the sensitivity analysis, performed on a one-cell, non-distributed version of the Atirro watershed model, inform which model parameters are most important to constrain when applying SMR to similar regions. In the following sections, we discuss the variable effects of model parameters on the response variables used in the sensitivity analysis to inform (1) the choice of field-based measurements, and (2) the interpretation of modeled LUCC and climate change impacts on watershed hydrology.

4.2.1. Parameterization of Baseflow

As expected for a mostly forested watershed, groundwater contributions make up a greater proportion of streamflow in the modeled Atirro watershed than runoff (Table 5), so parameters connected to that hydrological pathway (i.e., baseflow) are more sensitive. Groundwater discharge depends on available soil and aquifer storage. Consequently, the speed at which water exits the soil water reservoir (macropore K_{sat}) can greatly affect the magnitude and duration of the lowest simulated baseflow levels. Since soil depth, porosity, rock content and residual moisture content affect how much space in the soil is available for water storage and how much water remains after draining, they impart an influence on baseflow as well. Although K_{sub} influences the percolation to the deeper groundwater reservoir, in our analysis, its role appears less influential on low streamflow amounts and duration than soil water storage (soil depth, porosity, rock content, and residual moisture content) and the maximum lateral flow rate (macropore K_{sat}). Thus, low flow simulation in data-poor regions can be more accurately simulated with the aid of plot-scale measurements of soil porosity, rock content, soil depth and, particularly, macropore K_{sat} .

4.2.2. Parameterization of Peak Flows

Confidence in accurately simulating peak flows can be improved by validating the K_{sub} and macropore K_{sat} rates, soil depth, and porosity (Table 4). Heavy rainfall contributes to baseflow in all model iterations. Whereas this baseflow represents deeper percolation (K_{sub}) contributions to peak flow, peak flows and peak flow duration are also sensitive to shifts in the parameters dictating shallow subsurface soil storage and saturation-excess runoff: porosity, soil depth, and macropore K_{sat} . Supported by field observations of macropore contributions along channel banks during storm events, it is logical that the flow peaks in the forested scenario are dependent on lateral soil water flow as noted in similar environments at the plot-scale by Spaans et al. [22], Hanson et al. [20], and Toohey et al. [23]. Welsh et al. [42] identified high spring discharge contributions during heavy rainfall events in a neighboring Costa Rican watershed. Although not explicitly modeled here, spring outflow is likely activated during peak flows in our study watersheds as well. Based on the mass balance, the volume of baseflow greatly outweighs saturated excess runoff, except when a restrictive soil layer is present (Table 5), emphasizing the importance of appropriately simulating baseflow contribution.

In summary, application of SMR in the humid tropics should consider approaches to estimate macropore K_{sat} , K_{sub} , porosity, and soil depth. Macropore K_{sat} , K_{sub} , porosity, and soil depth should be measured directly in the target watershed to capture a representative range of values across different soil types and topographic settings if accurately simulating low flows is a modeling priority. Soil matrix K_{sat} is less important to measure directly since it weakly influences all response variables (Table 4), largely because at soil moisture levels between field capacity and saturation, the model defines hydraulic conductivity based on macropore K_{sat} ; the soil matrix K_{sat} parameter is only directly applied to calculating the effective hydraulic conductivity when soil water storage falls below field capacity. Lastly, the effects of impermeable surfaces (if present) and springs are also important to parameterize, and direct field measurements may enhance model performance.

4.3. Land Use and Climate Change Influence on Hydrology

Model simulations show that deforestation affects the response of tropical mountain watershed hydrology in our study region more severely than climate change (Figure 9). The sum of the 24 top discharge values from each of the rainfall intensity and amount scenarios in both forested and pasture-converted (without a hydraulically restrictive layer) scenarios shows that a forested watershed buffers the effect of altered rainfall intensity and amount whereas the pasture-converted watershed accentuates this effect. The effect of increased rainfall intensity is particularly amplified by conversion to pasture, increasing the sum of the annual peak discharges an average of 2094 m³/s relative to forest land cover that shows an average increase of only 94 m³/s. Simulated annual precipitation amount

increases from 70% to 110% show a similar land cover effect, raising the top discharge sum an average of 355–436 m³/s in forest versus 703–2344 m³/s in pasture for all rainfall intensity and temperature scenarios. These results suggest that intensive land use greatly increases delivery of precipitation to the channel network relative to forested watersheds. Field observations along pasture, sugar cane fields, and roads in the study watersheds corroborate this modeled result (Figure 1). Effects on stream hydrology due exclusively to increased precipitation (intensity and amount) and temperature, while significant, appear of a lesser magnitude (Figure 9). Our simulations indicate that deforested land can increase peak flows, deepen troughs between peak flows, decrease infiltration and soil reservoir recharge, and increase overland flow. Field observations and hydrology modeling have shown similar LUCC effects elsewhere in the humid tropics [14,20,22,23,56,57].

The influence of LUCC, caused by associated changes in soil conditions, is most pronounced after simulated conversion of forest to pasture, particularly if a restrictive soil layer develops in association with the conversion (Figure 9). The humid tropical forested watersheds in this study exhibit significant soil and groundwater storage relative to pasture conversion scenarios. Simulated soil conditions associated with pasture conversion effectively reduce the connectivity of soil and groundwater reservoirs thereby generating greater peak flows followed by rapid returns to baseflow levels that can be lower than forested baseflow. This reduction is exacerbated if a hydraulically restrictive layer develops as observed in soils similar to the study watersheds [20,22] (Figures 5, 6 and 7c). While soil storage and baseflow contribute to lateral soil water flow, saturation-excess runoff, and flow convergence in a forested watershed, overland flow is a more prominent pathway in pasture-dominated watersheds (Table 5). Furthermore, although stream hydrographs can be flashy in steep, forested watersheds of the humid tropics, soil storage slows hillslope flow and thereby moderates the influx of water to channels, maintaining a more consistent flow regime relative to pasture-dominated watersheds.

Where forest cover and associated soils dominate, high vertical hydraulic conductivities direct most non-intercepted precipitation into storage (i.e., soil and subsurface reservoirs) via infiltration. Percolation from the soil storage reservoir to the stream channel as baseflow contributes the most to discharge in forested basins (Table 5). Soil macropore and subsurface saturated hydraulic conductivities thus control the groundwater transmission that sustains the forest soil buffering effect with slower soil flow path travel times relative to overland flow paths, effectively limiting peak flows and maintaining low flows. Our simulations suggest that macropore hydraulic conductivity likely drives much of the vertical subsurface delivery of water at the watershed scale in the forested study watersheds (see LowFlow and LowDuration, Table 4), as recorded in the neighboring plot scale study by Toohey et al. [23]. In Honduran forest plots with soil characteristics more comparable to our study watersheds, Hanson et al. [20] measured no lateral soil water flow, only vertical. If macropore hydraulic conductivity is cut off, particularly by land use practices and noted in plot-scale observations by Spaans et al. [22] and Hanson et al. [20], lateral flow and overland flow can deliver water to the channel network more quickly and without replenishing deeper soil and groundwater reservoirs (see [58]) (Table 5 and Figure 6). In conjunction with soil depth and horizonation, soil matrix and macropore hydraulic conductivities can also control a saturation-excess fill-and-spill-type runoff generation mechanism [59].

One critical implication of greater peak flows associated with LUCC is greater stream power capable of transporting more and larger sediment from channel bed and banks. Channel widening and/or channel incision can result from such hydraulic shifts [60]. Likewise, lower baseflow levels can have implications for habitat and human water needs, partially due to fine sediment deposition and low water availability [61,62].

4.4. Hydrological Resilience to a Changing Climate

Cutting off subsurface storage and amplifying surface and near surface flow paths associated with pasture and sugar cane LUCC [20,22,23] shortens the watershed response time during precipitation events (Figures 5–7), and consequently the resilience of these

systems to climate change. Moreover, forested land can effectively buffer the impact of predicted increased rainfall intensities and extended dry periods (Figure 7a) in addition to reducing overland flow and associated soil erosion. It is also valuable to distinguish the influence of increased temperatures and associated *ET* loss from changes in discharge and flow timing. Based on the mass balance, more saturation-excess runoff exited the pasture watershed than the forested scenario (23 cm/basin/yr more; 192 cm/basin/yr more in pasture with a restrictive layer), resulting in greater peak flows from the pasture scenarios (Figure 9). However, a similar magnitude of additional annual *ET* loss (21 cm/basin/yr) in both land cover scenarios under an extreme temperature increase of +4 °C did not greatly impact the peak flows relative to precipitation intensity, amount, and particularly LUCC. Above all, forest conversion fundamentally alters the hydrologic state of these systems, more so if a hydraulically restrictive soil layer develops. The shift to pasture and other land use that restricts infiltration pathways sets up a situation in which both climate change and altered watershed hydrology reinforce a response characterized by greater runoff peaks separated by longer and more severe baseflow troughs. As a result, increased rainfall intensity as predicted for the tropics [7,8] can be expected to generate a relatively greater effect on pasture- and sugar-cane-dominated watersheds in the mountainous humid tropics than forested or agro-forested basins (Figures 5–7) [23]. However, it should be noted that (1) the spatial scope of our study is limited, focused on three regional watersheds that represent the humid tropics, and (2) the lack of stream gauge data for the Platanillo watershed, representing observed hydrology for a mixed land use/land cover watershed, prevents direct measurement of our simulated LUCC effects. Future studies should compare simulated and observed watershed hydrology as climate changes and LUCC occurs in monitored watersheds to measure the variable effects of land use and climate change. This would demonstrate how closely our simulations of changing watershed conditions match actual observations.

One key implication of our study underscores the opportunity for reforestation as a means to build resilience of these tropical watersheds to climate change impacts. Coupled human–natural system resilience is particularly difficult to estimate prior to disturbance (e.g., dry spells or extreme high precipitation events) in systems experiencing unprecedented trajectories. Even where long-term monitoring data exist, unprecedented climate conditions expected in the tropics [1] will impact landscapes undergoing intensifying land use, rendering past trends effectively irrelevant. These effects transfer into river channel hydrology, sediment transport and associated channel and floodplain morphology, spreading impacts downstream. Furthermore, communities in the study region depend on near-surface groundwater via springs for drinking water and expanding land development into unprotected recharge zones has the potential of limiting water availability as climate continues to shift [63]. It is possible, however, that reforestation can return the hydrology of these systems to their prior state if enough time is given for soils to reestablish their porous quality with the aid of deep and dense rooting [21,64]. The rapid natural vegetation growth rate in the humid tropics should support a return [65], but success depends on the time frame for redevelopment and reconnection of deep soil structure capable of storage and water transmission. Tools such as SMR that predict the effects of climate change on diverse landscapes under a variety of land cover scenarios can aid land managers planning for such non-stationary future conditions.

5. Conclusions

Our findings suggest that (1) the updated SMR model functions well and can thus be used to demonstrate the potential influences of changing environmental conditions, specifically LUCC and climate change, on watershed hydrology in the humid tropics, and (2) forest conversion more strongly influences watershed hydrology than modeled shifts in precipitation and temperature patterns associated with climate change in mountain watersheds of the humid tropics. Land development combined with intensifying precipitation events and increasing temperatures will likely increase hydrological variability. Significant decreases in soil infiltration and storage associated with deforestation can lead to increased

peak flow magnitude while flow duration and baseflow decrease. Conversely, reforestation can enhance the resilience of humid tropical watersheds to predicted increases in rainfall intensity and growing interannual climate variability, especially in mountainous terrain.

We demonstrate that a parsimonious, process-based spatially distributed hydrology model can provide valid, robust and meaningful results for interpreting the potential effects of land cover and climate change on watershed and stream hydrology, particularly in regions lacking long-term resource monitoring. Our modeling of hydrological processes in a region with minimal soil and hydrology data simulates watershed response and stream hydrology for spatially explicit land use conversion and climate scenarios without the need for extensive historic datasets or calibration. However, we show that peak flow simulation is most sensitive to input model parameter estimates dictating soil storage and both deep percolation and shallow subsurface pathways while low flow simulation is strongly influenced by macropore conductivity, soil depth, porosity, and field capacity moisture content. Where possible, these parameters should be field measured at the plot scale to constrain model simulations. Furthermore, for fluvial systems characterized by short, flashy flow regimes with relatively rapid flow concentration times such as the study watersheds, sub-daily time steps can better reproduce peak flow events at the cost of longer model run times.

Sustainable land and water resource development in the context of climate change requires insights provided by process-based modeling techniques. Future research focused on watershed dynamics in a changing environment should incorporate feedback mechanisms driven by watershed hydrology such as channel morphology, sediment transport, vegetation dynamics, and groundwater availability, into a more comprehensive model of watershed sensitivity and resilience.

Author Contributions: Conceptualization, T.J.; Methodology, J.B. and T.J.; Investigation, T.J. and A.K.F.; Writing—original draft, T.J.; Writing—review & editing, T.J., A.K.F. and J.B. All authors have read and agreed to the published version of the manuscript.

Funding: This work was funded by the National Science Foundation Integrated Graduate Education and Research Traineeship (IGERT) through the University of Idaho [Grant Number 0903479].

Data Availability Statement: The data that support the findings of this study are available from the corresponding author upon reasonable request.

Acknowledgments: We would like to acknowledge Frederico Gómez at the Instituto Costarricense de Electricidad for providing data from stream gauges and weather stations in the study region.

Conflicts of Interest: The authors declare no conflict of interest.

References

1. Mora, C.; Frazier, A.G.; Longman, R.J.; Dacks, R.S.; Walton, M.M.; Tong, E.J.; Sanchez, J.J.; Kaiser, L.R.; Stender, Y.O.; Anderson, J.M.; et al. The projected timing of climate departure from recent variability. *Nature* **2013**, *502*, 183–187. [[CrossRef](#)] [[PubMed](#)]
2. Wohl, E. Human impacts to mountain streams. *Geomorphology* **2006**, *79*, 217–248. [[CrossRef](#)]
3. Wohl, E.; Barros, A.; Brunsell, N.; Chappell, N.A.; Coe, M.; Giambelluca, T.; Goldsmith, S.; Harmon, R.; Hendrickx, J.M.H.; Juvik, J.; et al. The hydrology of the humid tropics. *Nat. Clim. Chang.* **2012**, *2*, 655–662. [[CrossRef](#)]
4. Karmalkar, A.V.; Bradley, R.S.; Diaz, H.F. Climate change scenario for Costa Rican montane forests. *Geophys. Res. Lett.* **2008**, *35*, L11702. [[CrossRef](#)]
5. Funk, C.C. *Drought, Flood, Fire: How Climate Change Contributes to Catastrophes*; Cambridge University Press: Cambridge, UK, 2021.
6. Magrin, G.O.; Marengo, J.A.; Boulanger, J.-P.; Buckeridge, M.S.; Castellanos, E.; Poveda, G.; Scarano, F.R.; Vicun, S. Central and South America. In *Climate Change 2014: Impacts, Adaptation, and Vulnerability. Part B: Regional Aspects. Contribution of Working Group II to the Fifth Assessment Report of the Intergovernmental Panel on Climate Change*; Barros, V.R., Field, C.B., Dokken, D.J., Mastrandrea, M.D., Mach, K.J., Bilir, T.E., Chatterjee, M., Ebi, K.L., Estrada, Y.O., Genova, R.C., et al., Eds.; Cambridge University Press: Cambridge, UK; New York, NY, USA, 2014; pp. 1499–1566.
7. Solomon, S.; Qin, D.; Manning, M.; Averyt, K.; Marquis, M. (Eds.) *Climate Change 2007—the Physical Science Basis: Working Group I Contribution to the Fourth Assessment Report of the IPCC*; Cambridge University Press: Cambridge, UK, 2007; Volume 4.
8. Stocker, T. (Ed.) *Climate Change 2013: The Physical Science Basis: Working Group I Contribution to the Fifth Assessment Report of the Intergovernmental Panel on Climate Change*; Cambridge University Press: Cambridge, UK, 2014.
9. Mahowald, N.M.; Ward, D.S.; Doney, S.C.; Hess, P.G.; Randerson, J.T. Are the impacts of land use on warming underestimated in climate policy? *Environ. Res. Lett.* **2017**, *12*, 094016. [[CrossRef](#)]

10. Ward, D.S.; Mahowald, N.M. Local sources of global climate forcing from different categories of land use activities. *Earth Syst. Dyn.* **2015**, *6*, 175–194. [[CrossRef](#)]
11. Nath, P.K.; Behera, B. A critical review of impact of and adaptation to climate change in developed and developing economies. *Environ. Dev. Sustain.* **2010**, *13*, 141–162. [[CrossRef](#)]
12. Salas, J.D.; Rajagopalan, B.; Saito, L.; Brown, C. Special Section on Climate Change and Water Resources: Climate Nonstationarity and Water Resources Management. *J. Water Resour. Plan. Manag.* **2012**, *138*, 385–388. [[CrossRef](#)]
13. Walker, B.; Salt, D. *Resilience Thinking: Sustaining Ecosystems and People in a Changing World*; Island Press: Washington, DC, USA, 2006.
14. Bruijnzeel, L. Hydrological functions of tropical forests: Not seeing the soil for the trees? *Agric. Ecosyst. Environ.* **2004**, *104*, 185–228. [[CrossRef](#)]
15. Harder, P.; Pomeroy, J.W.; Westbrook, C.J. Hydrological resilience of a Canadian Rockies headwaters basin subject to changing climate, extreme weather, and forest management. *Hydrol. Process.* **2015**, *29*, 3905–3924. [[CrossRef](#)]
16. Mao, F.; Clark, J.; Karpouzoglou, T.; Dewulf, A.; Buytaert, W.; Hannah, D. HESS Opinions: A conceptual framework for assessing socio-hydrological resilience under change. *Hydrol. Earth Syst. Sci.* **2017**, *21*, 3655–3670. [[CrossRef](#)]
17. Nadeau, T.-L.; Rains, M.C. Hydrological Connectivity Between Headwater Streams and Downstream Waters: How Science Can Inform Policy1. *JAWRA J. Am. Water Resour. Assoc.* **2007**, *43*, 118–133. [[CrossRef](#)]
18. Bruijnzeel, L.A. *Hydrology of Moist Tropical Forest and the Effects of Conversion: A State of Review*; UNESCO: Paris, France; Vrije Universiteit: Amsterdam, The Netherlands, 1991.
19. Germer, S.; Neill, C.; Krusche, A.V.; Elsenbeer, H. Influence of land-use change on near-surface hydrological processes: Undisturbed forest to pasture. *J. Hydrol.* **2010**, *380*, 473–480. [[CrossRef](#)]
20. Hanson, D.L.; Steenhuis, T.S.; Walter, M.F.; Boll, J. Effects of soil degradation and management practices on the surface water dynamics in the Talgua River Watershed in Honduras. *Land Degrad. Dev.* **2004**, *15*, 367–381. [[CrossRef](#)]
21. Niemeyer, R.; Fremier, A.; Heinse, R.; Chávez, W.; DeClerck, F. Woody Vegetation Increases Saturated Hydraulic Conductivity in Dry Tropical Nicaragua. *Vadose Zone J.* **2014**, *13*, vzi2013.01.0025. [[CrossRef](#)]
22. Spaans, E.J.A.; Baltissen, G.A.M.; Bouma, J.; Miedema, R.; Lansu, A.L.E.; Schoonderbeek, D.; Wielemaker, W.G. Changes in physical properties of young and old volcanic surface soils in Costa Rica after clearing of tropical rain forest. *Hydrol. Process.* **1989**, *3*, 383–392. [[CrossRef](#)]
23. Toohey, R.C.; Boll, J.; Brooks, E.S.; Jones, J.R. Effects of land use on soil properties and hydrological processes at the point, plot, and catchment scale in volcanic soils near Turrialba, Costa Rica. *Geoderma* **2018**, *315*, 138–148. [[CrossRef](#)]
24. Costa, M.H.; Botta, A.; Cardille, J.A. Effects of large-scale changes in land cover on the discharge of the Tocantins River, Southeastern Amazonia. *J. Hydrol.* **2003**, *283*, 206–217. [[CrossRef](#)]
25. McDonnell, J.J.; McGlynn, B.; Vache, K.; Tromp-Van Meerveld, I. A perspective on hillslope hydrology in the context of PUB, In Predictions in Ungauged Basins: International Perspectives on the State of the Art and Pathways Forward. In Proceedings of the Predictions in Ungauged Basins (PUB) Workshop, Perth, Australia, 2–5 February 2004; IAHS Publication: Wallingford, UK, 2005; Volume 301, pp. 204–212.
26. Mulligan, M. WaterWorld: A self-parameterising, physically based model for application in data-poor but problem-rich environments globally. *Hydrol. Res.* **2012**, *44*, 748–769. [[CrossRef](#)]
27. Boll, J.; Brooks, E.S.; Campbell, C.R.; Stockle, C.O.; Young, S.K.; Hammel, J.E.; McDaniel, P.A. Progress toward Development of a GIS based Water Quality Management Tool for Small Rural Watersheds: Modification and Application of a Distributed Model. Paper 982230. In Proceedings of the ASAE Annual International Meeting, Orlando, FL, USA, 12–16 July 1998.
28. Brooks, E.S.; Boll, J.; McDaniel, P.A. Distributed and integrated response of a geographic information system-based hydrologic model in the eastern Palouse region, Idaho. *Hydrol. Process.* **2006**, *21*, 110–122. [[CrossRef](#)]
29. Frankenberger, J.R.; Brooks, E.S.; Walter, M.F.; Steenhuis, T.S. A GIS-based variable source area hydrology model. *Hydrol. Process.* **1999**, *13*, 805–822. [[CrossRef](#)]
30. Yourek, M.; Brooks, E.S.; Brown, D.J.; Poggio, M.; Gasch, C. Development and application of the soil moisture routing (SMR) model to identify subfield-scale hydrologic classes in dryland cropping systems using the Budyko framework. *J. Hydrol.* **2019**, *573*, 153–167. [[CrossRef](#)]
31. Zhao, M.; Boll, J.; Brooks, E.S. Evaluating the effects of timber harvest on hydrologically sensitive areas and hydrologic response. *J. Hydrol.* **2020**, *593*, 125805. [[CrossRef](#)]
32. Ticehurst, J.; Cresswell, H.; McKenzie, N.; Glover, M. Interpreting soil and topographic properties to conceptualise hillslope hydrology. *Geoderma* **2007**, *137*, 279–292. [[CrossRef](#)]
33. Pérez, C.F.B. Análisis Multitemporal de Cambio de uso de Suelo y Dinámica del Paisaje en el Corredor Biológico Volcánica Central Talamanca, Costa Rica. Masters Thesis, CATIE, Turrialba, Costa Rica, 2009; 124p.
34. Instituto Mexicano de Tecnología del Agua. *Elaboración de Balances Hídricos por Cuencas Hidrográficas y Propuesta de Modernización de las Redes de Medición en Costa Rica*; BID: San José, Costa Rica, 2008.
35. UNESCO Office Montevideo and Regional Bureau for Science in Latin America and the Caribbean. *Balance Hídrico Superficial de Costa Rica, Período 1970–2002*; Documento Técnico del PHI-LAC; UNESCO: Montevideo, Uruguay, 2007; 55p.
36. Winowiecki, L.; McDaniel, P.A.; Mata, R.; Jones, J.J. Constructing a soil map for the coffee-dominated region of Turrialba, Using GIS. In Proceedings of the Fifth Annual meeting of the University of Idaho and CATIE IGERT Project, Moscow, ID, USA, 16–19 May 2007; pp. 101–102.

37. Bergoeing, J.P.; Malavassi, E. *Geomorphological Map of the Central Valley of Costa Rica*, in 1:50,000; Instituto Geográfico Nacional: San José, Costa Rica, 1982.
38. Jansson, M.B. Determining sediment source areas in a tropical river basin, Costa Rica. *Catena* **2002**, *47*, 63–84. [[CrossRef](#)]
39. Mora Cordero, I. Evaluación de la Pérdida de Suelo Mediante la Ecuación Universal (EUPS): Aplicación Para Definir Acciones de Manejo en la Cuenca del Río Pejibaye, Vertiente Atlántica, Costa Rica. Masters Thesis, Universidad de Costa Rica, San José, Costa Rica, 1987; 104p.
40. Torres, J.A. Estudio de suelos. In *Estudio Geoagronómico de la Región Oriental de la Meseta Central*; Dóndoli, C., Torres, J.A., Eds.; Ministerio de Agricultura e Industrias: San José, Costa Rica, 1952; pp. 107–175.
41. Allen, R.G.; Pereira, L.S.; Raes, D.; Smith, M. *Crop Evapotranspiration—Guidelines for Computing Crop Water Requirements—FAO Irrigation and Drainage Paper 56*; FAO: Rome, Italy, 1998; Volume 300, p. D05109.
42. Welsh, K.; Boll, J.; Sánchez-Murillo, R.; Rouspard, O. Isotope hydrology of a tropical coffee agroforestry watershed: Seasonal and event-based analyses. *Hydrol. Process.* **2018**, *32*, 1965–1977.
43. Keller, C.K.; van der Kamp, G.; Cherry, J.A. Fracture permeability and groundwater flow in clayey till near Saskatoon, Saskatchewan. *Can. Geotech. J.* **1986**, *23*, 229–240. [[CrossRef](#)]
44. Keller, C.; Van Der Kamp, G.; Cherry, J. Hydrogeology of two Saskatchewan tills, I. Fractures, bulk permeability, and spatial variability of downward flow. *J. Hydrol.* **1988**, *101*, 97–121. [[CrossRef](#)]
45. Tallaksen, L.M. A review of baseflow recession analysis. *J. Hydrol.* **1995**, *165*, 349–370. [[CrossRef](#)]
46. Nash, J.E.; Sutcliffe, J.V. River flow forecasting through conceptual models part I—A discussion of principles. *J. Hydrol.* **1970**, *10*, 282–290. [[CrossRef](#)]
47. Moriasi, D.N.; Arnold, J.G.; van Liew, M.W.; Bingner, R.L.; Harmel, R.D.; Veith, T.L. Model evaluation guidelines for systematic quantification of accuracy in watershed simulations. *Trans. ASABE* **2007**, *50*, 885–900. [[CrossRef](#)]
48. Foglia, L.; Hill, M.C.; Mehl, S.W.; Burlando, P. Sensitivity analysis, calibration, and testing of a distributed hydrological model using error-based weighting and one objective function. *Water Resour. Res.* **2009**, *45*, W06427. [[CrossRef](#)]
49. Guinot, V.; Gourbesville, P. Calibration of physically based models: Back to basics? *J. Hydroinformatics* **2003**, *5*, 233–244. [[CrossRef](#)]
50. Harper, E.B.; Stella, J.; Fremier, A.K. Global sensitivity analysis for complex ecological models: A case study of riparian cottonwood population dynamics. *Ecol. Appl.* **2011**, *21*, 1225–1240. [[CrossRef](#)]
51. Breiman, L. Random forests. *Mach. Learn.* **2001**, *45*, 5–32. [[CrossRef](#)]
52. Hamon, W.R. Estimating Potential Evapotranspiration. *J. Hydraul. Div.* **1961**, *87*, 107–120. [[CrossRef](#)]
53. Welsh, K. Hydrologic Processes and Water Resource Management of Tropical Watersheds: An Interdisciplinary Study in Costa Rica. Ph.D. Thesis, University of Idaho, Moscow, ID, USA, 2015; 137p.
54. Brutsaert, W. *Hydrology*; Cambridge University Press: Cambridge, UK, 2005.
55. Montero, P.W.; Lewis, J.C.; Marshall, J.S.; Kruse, S.; Wetmore, P. Neotectonic faulting and forearc sliver motion along the Atirro-Rio Sucio fault system, Costa Rica, Central America. *GSA Bull.* **2013**, *125*, 857–876. [[CrossRef](#)]
56. Jones, J.A.; Grant, G.E. Peak Flow Responses to Clear-Cutting and Roads in Small and Large Basins, Western Cascades, Oregon. *Water Resour. Res.* **1996**, *32*, 959–974. [[CrossRef](#)]
57. Lamparter, G.; Nobrega, R.; Kovacs, K.; Amorim, R.S.S.; Gerold, G. Modelling hydrological impacts of agricultural expansion in two macro-catchments in Southern Amazonia, Brazil. *Reg. Environ. Chang.* **2018**, *18*, 91–103. [[CrossRef](#)]
58. Schellekens, J.; Scatena, F.N.; Bruijnzeel, L.A.; van Dijk, A.I.J.M.; Groen, M.M.A.; van Hogezaand, R.J.P. Stormflow generation in a small rainforest catchment in the Luquillo Experimental Forest, Puerto Rico. *Hydrol. Process.* **2004**, *18*, 505–530. [[CrossRef](#)]
59. Toohey, R. Land Use, Hydrological Processes and Ecosystem Services in the Upper Reventazón Watershed, Costa Rica. Ph.D. Thesis, University of Idaho, Moscow, ID, USA, 2012.
60. Schumm, S.A. Causes and controls of channel incision. In *Incised River Channels, Processes, Forms, Engineering and Management*; Darby, S.E., Simon, A., Eds.; John Wiley & Sons: Chichester, UK, 1999; pp. 19–33.
61. Poff, N.L.; Allan, J.D.; Bain, M.B.; Karr, J.R.; Prestegard, K.L.; Richter, B.D.; Sparks, R.E.; Stromberg, J.C. The Natural Flow Regime. *Bioscience* **1997**, *47*, 769–784. [[CrossRef](#)]
62. Wood, P.J.; Armitage, P.D. Sediment deposition in a small lowland stream—Management implications. Regulated Rivers: Research & Management. *Int. J. Devoted River Res. Manag.* **1999**, *15*, 199–210. [[CrossRef](#)]
63. Welsh, K.; Keesecker, L.; Hill, R.; Joyal, T.; Boll, J.; Bosque-Pérez, N.A.; Cosens, B.; Fremier, A.K. Scale mismatch in social-ecological systems: A Costa Rican case study of spring water management. *Sustain. Water Resour. Manag.* **2020**, *6*, 40.
64. Hassler, S.K.; Zimmermann, B.; van Breugel, M.; Hall, J.S.; Elsenbeer, H. Recovery of saturated hydraulic conductivity under secondary succession on former pasture in the humid tropics. *For. Ecol. Manag.* **2011**, *261*, 1634–1642. [[CrossRef](#)]
65. Chazdon, R.L.; Broadbent, E.N.; Rozendaal, D.M.; Bongers, F.; Zambrano, A.M.A.; Aide, T.M.; Balvanera, P.; Becknell, J.M.; Boukili, V.; Brancalion, P.H.; et al. Carbon sequestration potential of second-growth forest regeneration in the Latin American tropics. *Sci. Adv.* **2016**, *2*, e1501639. [[CrossRef](#)]

Disclaimer/Publisher’s Note: The statements, opinions and data contained in all publications are solely those of the individual author(s) and contributor(s) and not of MDPI and/or the editor(s). MDPI and/or the editor(s) disclaim responsibility for any injury to people or property resulting from any ideas, methods, instructions or products referred to in the content.